Bollettino di Geofisica Teorica ed Applicata Vol. 54, n. 3, pp. 245-256; September 2013
DOI 10.4430/bgta0102

Investigation of the electrical resistivity and geological structures on the hot springs in Markazi province of Iran using magnetotelluric method

B. Oskooi[1], M. Darijani[1] and M. Mirzaei[2]

[1] *Institute of Geophysics, University of Tehran, Iran*
[2] *Department of Physics, Faculty of Sciences, University of Arak, Iran*

(Received: October 20, 2012; accepted: May 6, 2013)

ABSTRACT The Mahalat region of Markazi province in Iran is a popular tourist spot due to the occurrence of hot springs and having the greatest geothermal fields in Iran. We chose a 6 km profile with 12 sites across the hot springs for carrying out a magnetotelluric (MT) survey on July 2011. A 2D inversion was applied on the determination MT data to resolve the subsurface conductive structures using a 2D inversion routine of Occam approach. The 2D model significantly illustrates the geothermal structures at depth, including cap rock (from 100 to 600 m), reservoir (from 500 to 2000 m) and the heat source (starting from 1000 m), and it shows a good correlation with the geological features. One of the interesting results is distinguishing the main faults, which are acting as the preferential paths to circulate the hydrothermal fluids. The resistivity model fits on the geological section along the MT profile.

Key words: electrical conductivity, geothermal, hot springs, magnetotelluric, Markazi province, 2D inversion.

1. Introduction

The magnetotelluric (MT) method is a passive electromagnetic (EM) technique that uses the natural, time varying electric and magnetic field components measured at right angles at the surface of the Earth to make inferences about the Earth's electrical structure, which, in turn, can be related to geology, tectonics and subsurface conditions. Measurements of the horizontal components of the natural electromagnetic field are used to construct the full complex impedance tensor, *Z*, as a function of frequency. The determinant of impedance tensor (*ZDET*), which is also called the effective impedance (Pedersen and Engels, 2005), is defined as

$$ZDET = (ZxxZyy - ZxyZyx)^{1/2}. \quad (1)$$

Using the effective impedance, determinant apparent resistivities and phases are computed. The advantage of using the determinant data is that it provides a useful average of the impedance for all current directions. The determinant apparent resistivities and phases are used for the inversion.

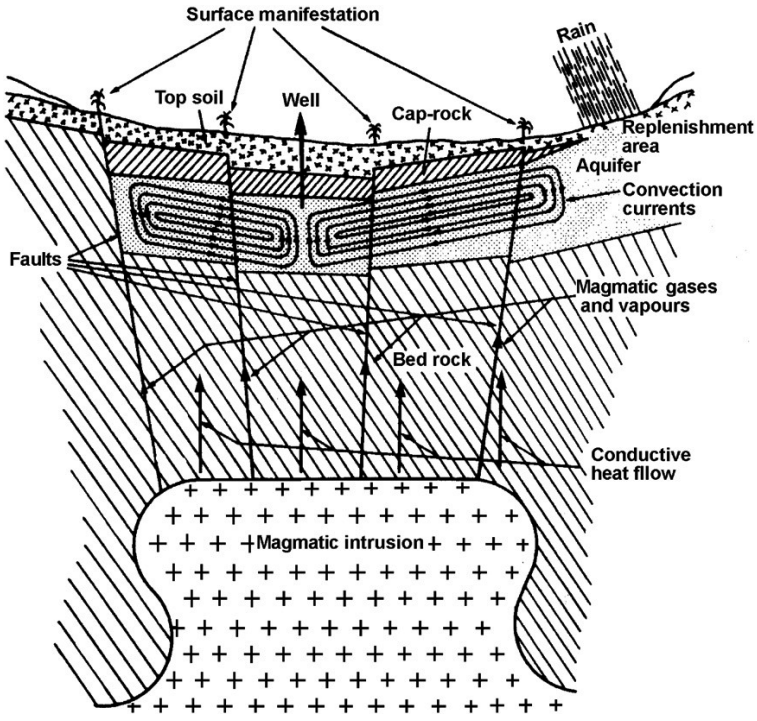

Fig. 1 - Conceptual model of a hyper-thermal field (Berktold, 1983).

MT method has been proved to be useful for widespread applications. For example, MT is extensively being used in imaging the fluids in subduction zones and volcanic belts (Wannamaker *et al.*, 1989; Jones and Dumas, 1993; Unsworth *et al.*, 1997, 1999), orogenic regions (Jones *et al.*, 1997; Unsworth, 2010), delineation of ancient and modern subduction zones (Jones, 1993; Naganjaneyulu and Santosh, 2010 and references therein), lithospheric studies (Campbell, 1978; Jones *et al.*, 2003; Patro and Sarma, 2009) and geothermal studies (Johnston *et al.*, 1992; Spichak and Manzella, 2009). MT can constrain the fluid content and thermal structure, which are the key parameters for defining the rheology of the crust and upper mantle (Unsworth, 2010).

Geothermal resources are ideal targets for EM methods since they produce strong variations in underground electrical resistivity. In geothermal areas, the electrical resistivity is substantially different from and generally lower than in areas with colder subsurface temperature (Oskooi *et al.*, 2005). Moreover, the penetration water in Earth cracks produces a reduction of the bulk resistivity, and makes the fault detecting easier than in other place. Fig. 1 reports a conceptual model showing the main elements of this type of geothermal system (Berktold, 1983).

An MT pilot study is used to investigate the structure of the geothermal field located in the Markazi province in central Iran. Previous studies suggest that the heat of hot springs is related to the heat from the cooling of molten magma and also the water of hot springs are formed from meteoric waters mixing with magmatic waters (Beitollahi, 1996; Oskooi and Darijani, 2013). Hydrology and geochemistry studies (Rezaie *et al.*, 2009) showed that the average temperature of the hot springs are about 46°C and their pH ranges from acidic to neutral. The estimated temperature of the geothermal reservoir is about 100°C. The water of hot springs is saturated by calcite minerals, hinting that the geothermal reservoir is probably formed of limestones.

Currently the main usage of the hot springs is as tourism attraction as well as health treatment. But, considering the high flow rate and temperature of the hot springs, there exist a potential for the hydrothermal energy purposes.

2. Geological setting

Geological structures in the Markazi province are characterized by a dextral rotational movement caused by the northward underthrusting of the Arabian plate beneath the Iranian plate (McKenzie, 1972). Due to this tectonic framework, the Cenozoic geologic history and the stratigraphy of the region are complex, with units of different structural characteristics. Igneous activities took place in the Eocene with the accumulation of volcanic rocks over a sequence of Mesozoic and Paleozoic sediments. These rocks were thermally metamorphosed by an Early Miocene monzonitic batholith, which is elongated in a NW-SE direction.

The area of study is located on the central Iran (CI) zone and Sanandaj-Sirjan metamorphic Zone (SSZ). A lot of faults pass through the region and divide it into blocks. In the geological dividing of Iran, the Mahalat area is located in the volcanic zone of CI. This zone has been one of the active and energetic zones during the different geological periods. This area, considering its permeability related to the expansion of calcareous and dolomite units and also the presence of cracks and joints, is potentially well suited to be a geothermal reservoir while the heat sources are located not very deep. The faults and cracks drain the water circulation in the region. Fig. 2 shows the geological setting and the position of the hot springs in travertines, shales and sandstones. The outcropping formations include: Shemshak with the lithology of shale and sandstone related to Jurassic age, orbitolina limestone unit related to Cretaceous age, Qom formation with marly limestone unit related to Miocene age and within these formations outcrops of igneous rocks including granodiorite, tuff and lava also exist in the region, showing that the last volcanic activities occurred in Eocene. Thermal fluids upflow from the travertine deposits and alluvia.

3. MT data acquisition and analysis

Prospecting in the Markazi geothermal area was aimed at delineating the boundary of the promising zone, imaging out the subsurface resistivity structure associated with the sedimentary alteration zone and the underlying reservoir as well as recognizing the fault system.

The MT survey was carried out at 12 stations covering the western zone of hot spring. The survey was designed using a profile system with interval stations of 500 m. The approximately E-W oriented faults indicate a general 2D subsurface structure and allow for an MT survey organized along a profile as a first approximation. The topography relief is low so that we could ignore the altitude differences (a maximum of 100 m) between MT sites. The possible EM noise is originated from human activities in the southern part of the survey area.

The survey was carried out using GMS05 (Metronix, Germany) systems in July 2011. Data were stored on an internal hard disk and downloaded via a connection to the field laptops. Power was supplied by a 12 V external battery. Three magnetometers and two electric dipoles were connected to five-channel data logger. For the registration of magnetic field variations in the

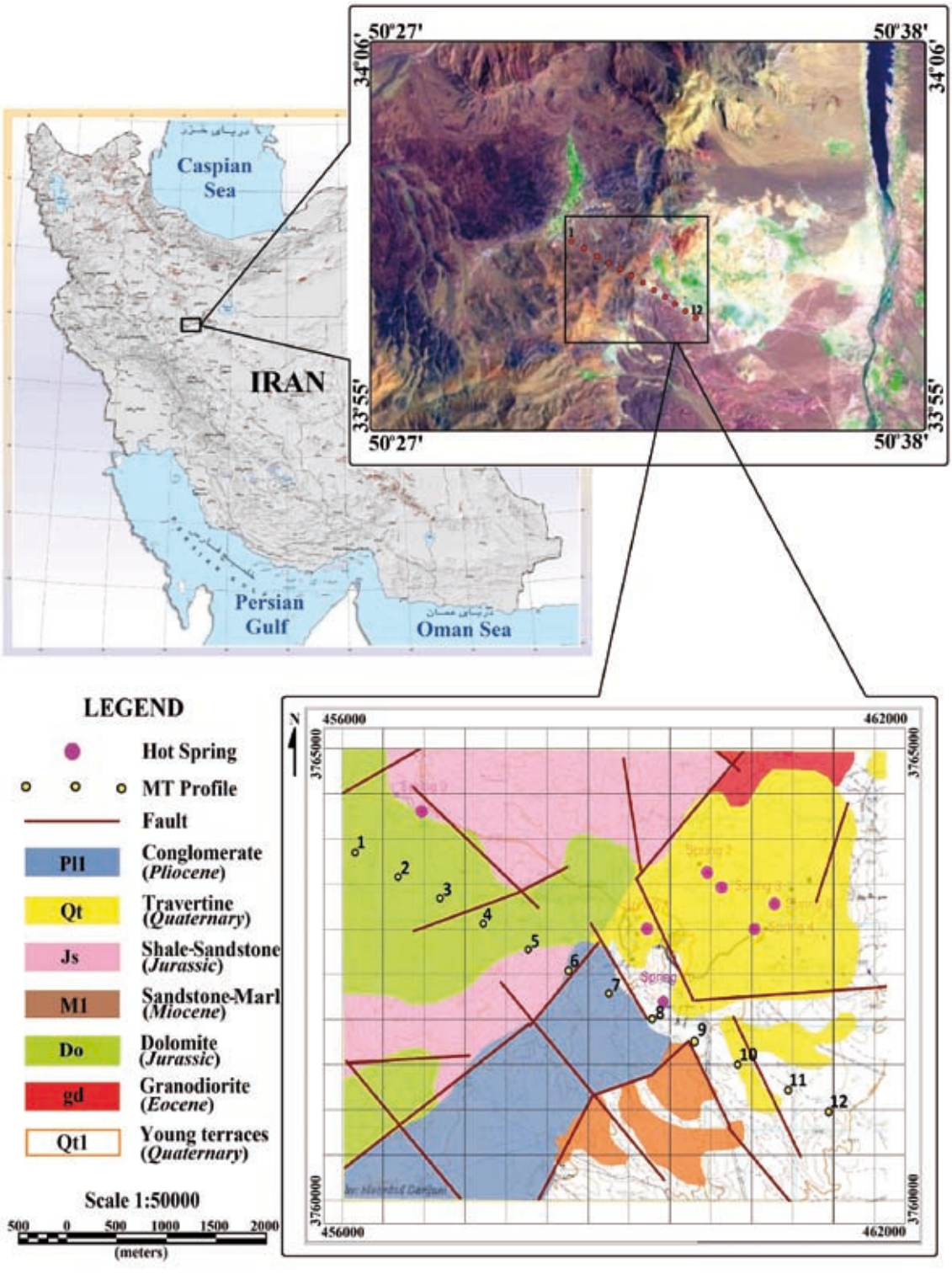

Fig. 2 - Study area in the Markazi province in Iran, a satellite picture and a large scale geological map with projected MT site locations.

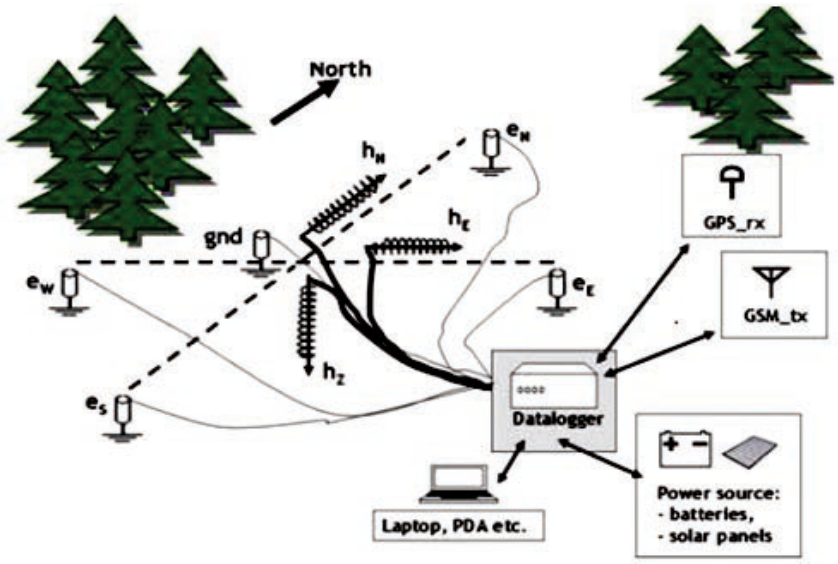

Fig. 3 - MT field array.

period range 0.0001 to 128.0 s broadband induction coil magnetometers were used. The electric field variations were registered by measuring potential differences between two couples of non-polarizable electrodes which were distributed at a distance of 100 m in N-S (E_x) and E-W (E_y) direction. Coupling to the soil was improved using water. The data logger and magnetometers were located in the centre, whereas the three induction coils were oriented N-S (H_x), E-W (H_y) and vertical (H_z) at a distance of 10 m from the data logger and at least 1 m from electric wires and 5 m from any conductive object. The vertical coil was buried to 4/5 of its length and covered by a plastic tube to avoid wind noises (Fig. 3).

A self-test including internal calibration was carried out automatically upon starting the measurement. Data in four period bands have been measured at each site: for each stack, the first band (period range 0.0001 - 0.004 s) with a sampling rate of 32768 Hz; the second band (period range 0.004 - 0.125 s) with a sampling rate of 4096 Hz; the third band (period range 0.125 - 4.0 s) with a sampling rate of 128 Hz and the fourth band (period range 4.0 - 128.0 s) with a sampling rate of 4 Hz. About 100 stacks and 30 stacks have been recorded for the first three bands and band 4, respectively. The average recording time needed at each measurement site was about 18 hours in total. Necessary items for the field campaign for instance note-book PC's, desktop PC's, compasses, hand-held GPS receivers, batteries, cables, mobile phones, 4WD cars, etc. were in service accordingly.

Time series measurements collected in various frequency ranges were transformed into frequency domain, and cross power spectra computed to estimate the impedance tensor as a function of frequency. Most of the MT data proved of reasonably good quality when processed by a code from Smirnov (2003) aiming at a robust single site estimate of EM transfer functions. To perform Fourier analysis the length of window was selected having 16384 samples with a 50% overlap with the neighboring windows. Coherency threshold was set to a high value (0.9), allowing extraction of enough highly coherent segments for further statistics. As the area of study was populated and close to urban noise sources, at the middle of the profile some recorded data did not show a good quality, as proved by the low coherency between the electric and

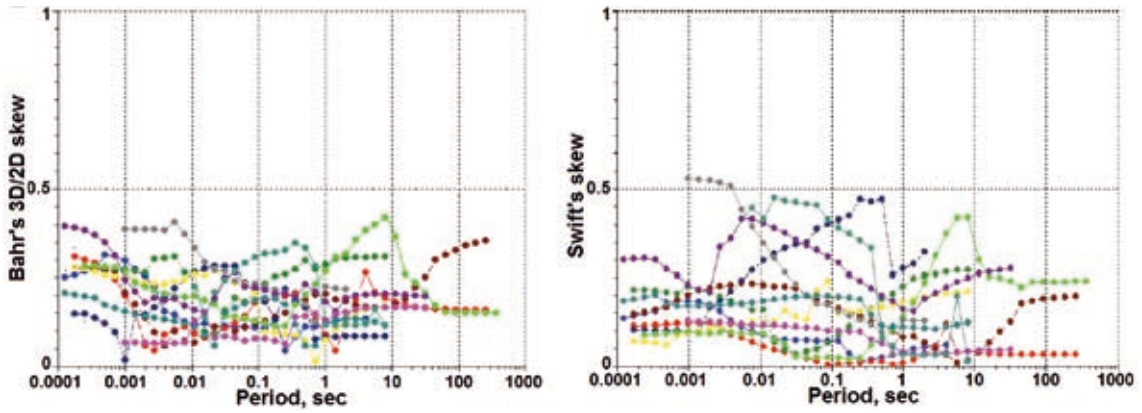

Fig. 4 - Bahr's 3D/2D skew (left pannel) and Swift's skew (right).

magnetic channels. As a result, some of the noisiest sites/frequencies were excluded from the database.

In order to estimate the dimensionality, the rotationally invariant parameter, Swift skew (Swift, 1967) is evaluated. Swift skew lies between 0 and 1 for real data and indicates deviations from 1D/2D conductivity distribution. However, it is sensitive to galvanic distortions (Bahr, 1988) due to small scale heterogeneities in the near surface and thus may give erroneous view on the dimensionality of the underlying medium (Smirnov and Pedersen, 2009). In contrast to the Swift skew, Bahr skew (Bahr, 1991) is insensitive to galvanic distortions and provides appropriate dimensionality with an assumption that for a regional 2D structure, the off-diagonal elements of impedance tensor must have the same phase. The small Swift skew (generally less than 0.3) for most of the sites indicates 2D condition, but there are several sites where Swift skew is rather large, thus indicating either 3D effects or near surface distortions (Dhanunjaya Naidu *et al.*, 2011). However, Bahr's phase sensitive skew is below 0.4 (Fig. 4) for the majority

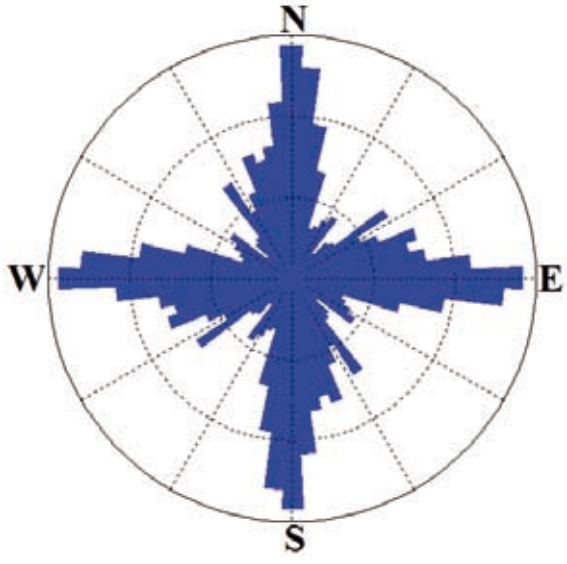

Fig. 5 - Rose diagram showing electrical strike direction. Calculations are made for the whole periods and sites.

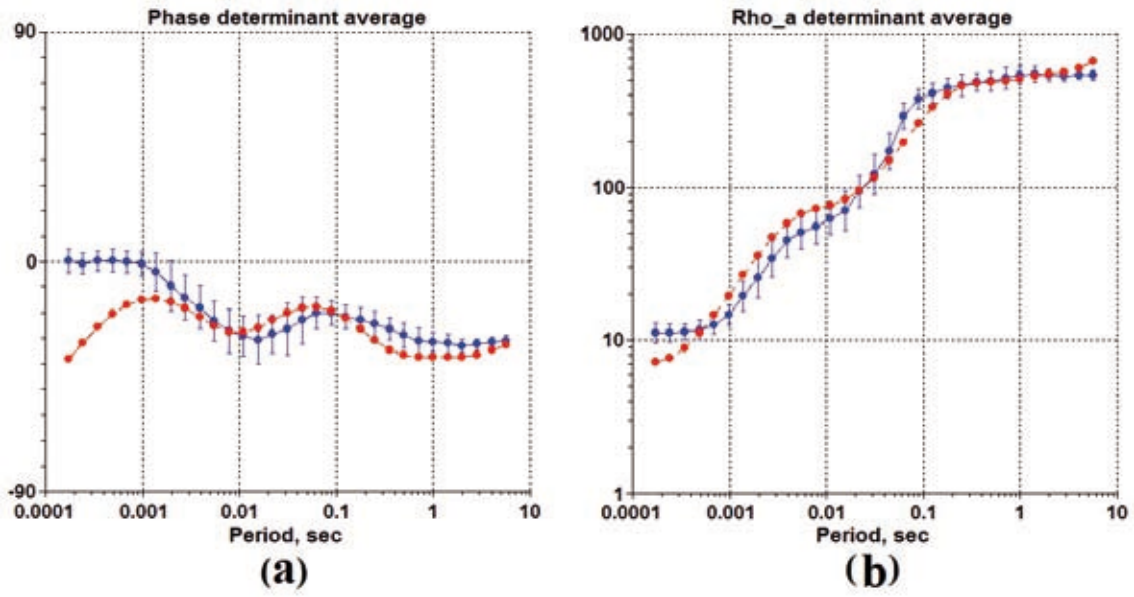

Fig. 6 - Phases (a) and apparent resistivities (b) of the determinant impedance for site 5 as an example. Blue points refer to the field data and red to the 1D model responses, respectively.

of sites, which means that high Swift skew values would be due to the presence of galvanic distortions and 2D condition was assumed for our data along the profile.

Regional strikes are calculated following the "phase tensor" scheme (Caldwell *et al.*, 2004). In this approach the phase relationship contained in MT impedance data is considered as a second rank tensor, "phase tensor". Decomposing the tensor to its SVD form, the orientation of the strike angle is determined as the direction that produces maximum or minimum impedance phases. Since there is no knowledge as to which of the maximum or minimum phases correspond to the polarization, a 90° ambiguity remains in determining the strike direction. In practice this ambiguity is resolved by the use of the vertical magnetic field data and considering the regional geological strikes (Montahaie *et al.*, 2010). Fig. 5 displays electric strike direction in a rose diagram for the profile and at all periods. The resolution of the rose diagram is 5 degrees. It yields an average strike direction of 0° for the profile. Accordingly the N-S direction would be identified as the major strike direction for the whole profile.

4. Inversion and interpretation

1D and 2D inversions are conducted to resolve the conductive structures. We applied a code from Pedersen (2004) for 1D inversion of the determinant data for all sites to resolve a reasonable starting model for 2D inversion scheme. Phases and apparent resistivities of the determinant impedance data and 1D model response are shown for site 5 in Fig. 6. Then we performed the 2D inversion of the determinant data using a code from Siripunvaraporn and Egbert (2000). It is worth to mention that since our MT data were collected in the period range 0.0001 - 128.0 s and knowing that the average bulk resistivity of the top layers is extremely low

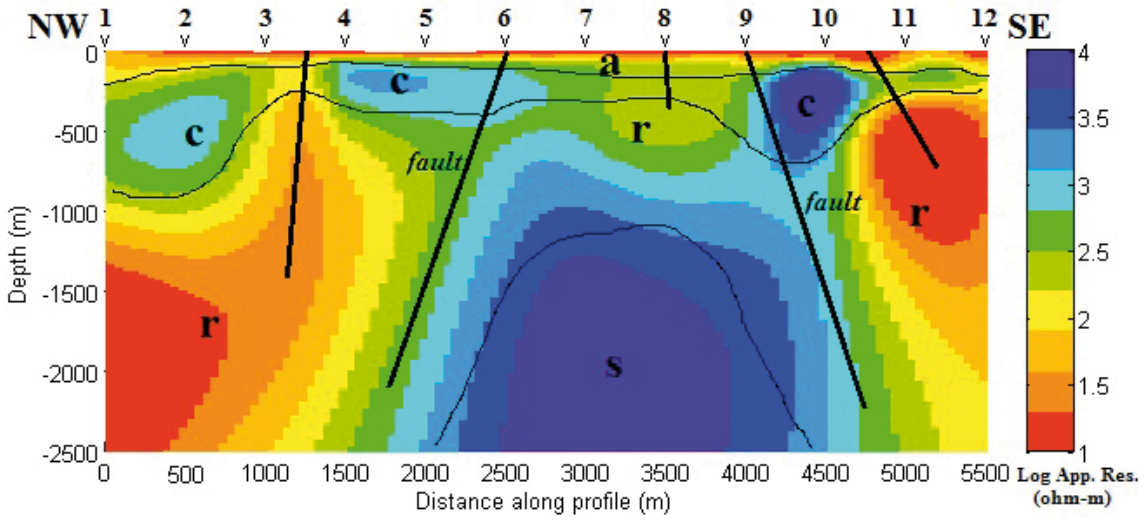

Fig. 7 - 2D inversion model of the DET-mode data.

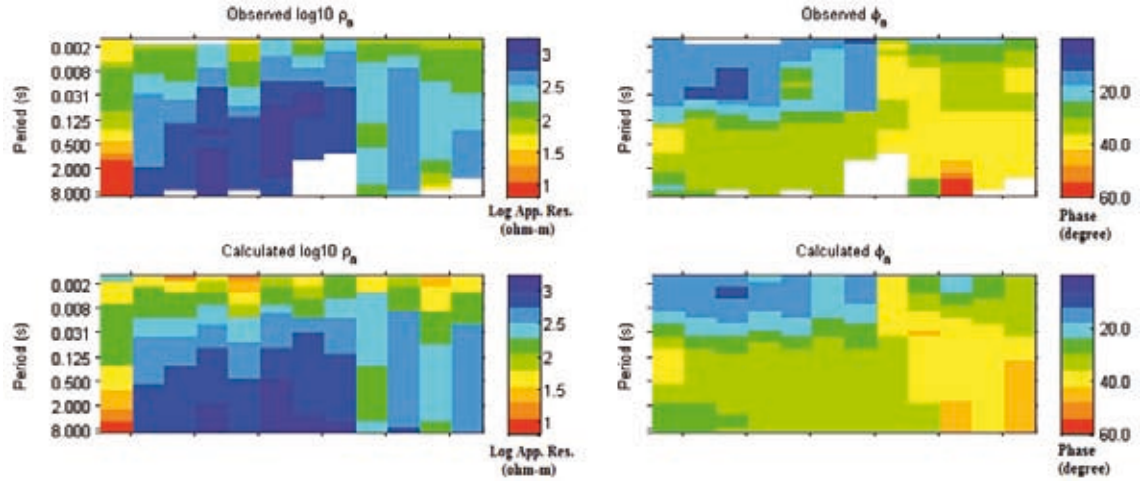

Fig. 8 - DET-mode data and responses of the 2D inversion.

(about 10 Ω·m) we consider a maximum skin depth of about 18 km for the region so that the effective depth penetration (roughly 1/5 of the skin depth) would be about 3.5 km. Our model is plotted down to 2.5 km. The resulting 2D model of the DET-mode data is shown in Fig. 7, and the field data and model data are shown in Fig. 8. To avoid probable unrealistic small errors on the data for the 2D approximation, an error floor of 15% on the apparent resistivity and 5% for the phase were used. Static shifts were corrected prior to the inversion based upon the DC resistivity information along the profile.

To get a better interpretation we show a 3D perspective of the surface geological map together with the final resistivity model along the MT profile in Fig. 9a. A geological section along the same profile is also depicted in Fig. 9b for an easy comparison. With due attention

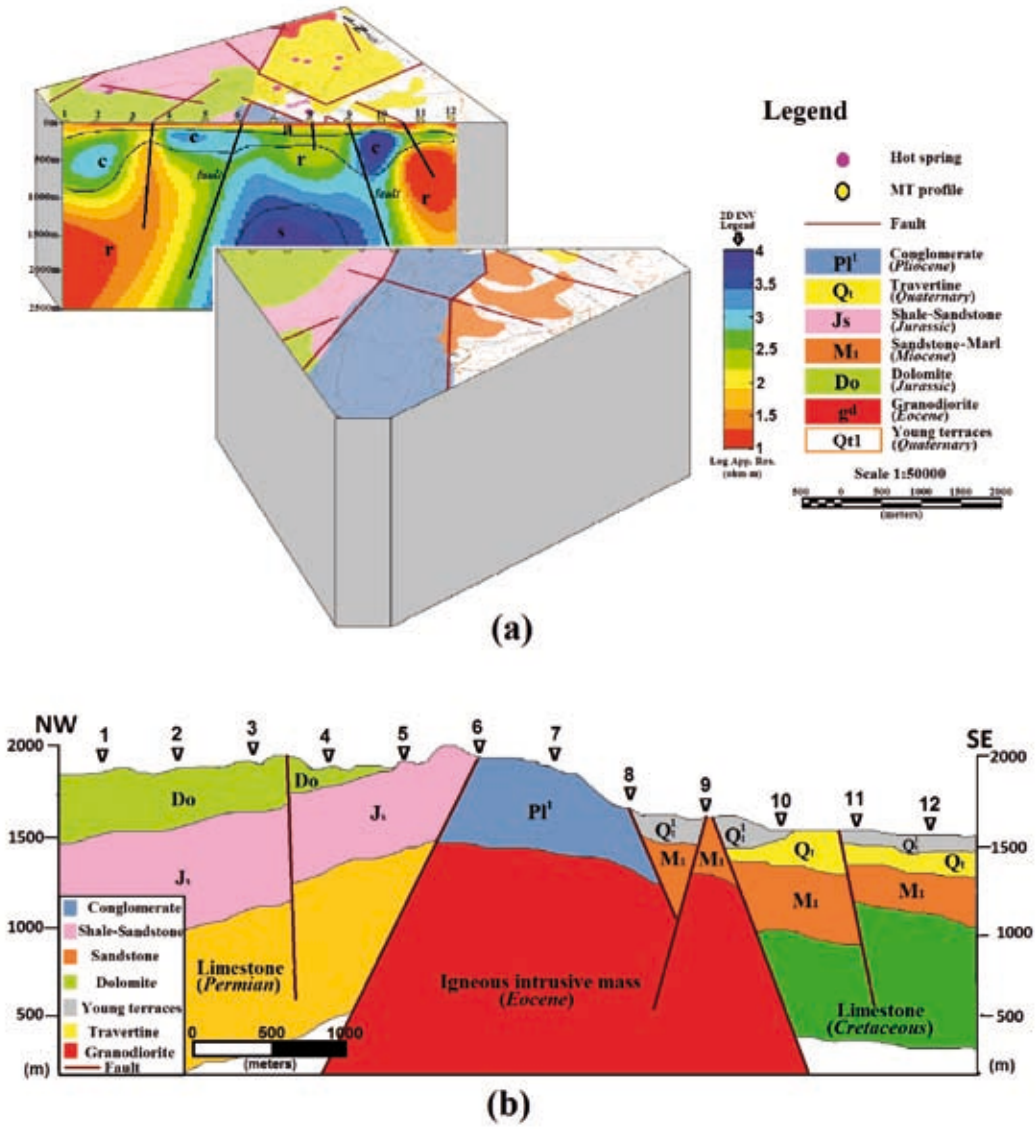

Fig. 9 - A 3D image of the combination of the geological map and the 2D resistivity model (a) and the geological profile corresponding to the MT profile (b).

to Figs. 7 and 9 we can obtain the results: from surface to about 100 m depth, the shallow conductive layer, (< 10 Ω·m) showing variable thickness along the profile, is most naturally interpreted as the zone penetrated by surface water due to cracks on the Earth surface (zone a). The surface is covered by clay and sand that is a good condition for water storage. Below this conductor along the whole of the MT profile, a resistive zone (~ 1000 Ω·m) is observed, which can be assigned to impermeable rocks such as shale and sandstone belonging to the Shemshak formation of Jurassic age for the north of profile, and Miocene sandstone and Quaternary travertine for the south of profile. These are interpreted as the cap-rock of the system (zone c). Below this resistive layer there is a conductive layer (< 10 Ω·m), showing variable thickness along the profile. It is interpreted as the Permian limestone for the north of profile and

Cretaceous limestone, for the south of profile (zone r) including hydrothermal circulations. Zone r acts as the system reservoir. Below this conductor in the middle of the profile below 1000 m depth, a very resistive zone is observed (> 1000 Ω·m). This resistive body is interpreted as the intrusive mass, which possibly acts as heat source of the geothermal system (zone s). Due to the tectonic framework, the last igneous activity occurred in Eocene. After the Eocene age the magmatic intrusion gradually got cold but in spite of the decreasing of heat in intrusive mass, the heat of this old magma is still available at depth in the area, possibly due also to radioactive decay effects (to be checked). The faults correspond to the conductive zones because of the penetration of the fluids in the cracks, highlighted by dark lines in Figs. 7 and 9, where they show a good correlation with geology. Faults and cracks drain the meteoric waters in the ground and also act as exit ways for the fluids coming from the reservoir to surface after heating by geothermal source. For example, around the two faults in Fig. 9 between the stations 10 and 11 and especially between the stations 3 and 4 these conductive features correspond to water upflows. Most of these faults are caused by tectonic activities but the faults and fractures in the stations 6 and 9 are probably due to the pressure of the uplift of magma intrusive mass. The results of our study indicate that an alteration zone is present beneath the surface; suggesting the existence of a hydrothermal fluid circulation at depth.

5. Conclusions

The geothermal field in the Markazi province of Iran is investigated using 12 MT stations data recorded on 2011 and distributed along a profile with elevation from 1657 to 1891 m, which were inverted by an Occam inversion routine. The resulting main features of the conductivity structures improved our understanding of the geological structures around the hot springs. The conductive layer at the surface can clearly be interpreted as the flows of the fluids in the fractures of the rocks and the top soil which is saturated with penetrated surface water. Hydrothermal fluids circulating through several main faults are represented as resistivity anomalies in the resistivity section, which image the active hydrothermal zone in the area. The 2D model significantly illustrates the geothermal structures including cap rock (from 100 to 600 m), reservoir (from 500 to 2000 m) and source (from 1000 m to the maximum investigation depth). We succeeded to map the geological structures beneath travertine cover around the hot springs. This study demonstrates how MT data can provide information about deep structures, which cannot always be achieved using other geophysical techniques.

Acknowledgements. The research council of the University of Tehran (UT) is acknowledged for the financial support of the first author's sabbatical leave at Uppsala University (UU) in the period of October 2011 to October 2012. The Department of the Earth Sciences of UU is also appreciated for hosting the first author as guest researcher. Arak University in Iran is appreciated for the financial support of the field work and also M. Montahaie and F. Ghadimi Aroos Mahalleh for useful guidance on the data processing and the geological information of the area, respectively. The authors also acknowledge the reviewers of the journal, A. Manzella and G. Santarato, for their precious points on the manuscript to become a paper.

REFERENCES

Bahr K.; 1988: *Interpretation of the magnetotelluric impedance tensor: regional induction and local telluric distortion*. J. Geophys., **62**, 119-127.

Bahr K.; 1991: *Geological noise in magnetotelluric data - a classification of distortion types*. Phys. Earth Planet. Inter., **66**, 24-38.

Beitollahi A.; 1996: *Travertine formation and the origin of the high natural radioactivity in the region of Mahallat hot springs*. The M.Sc. Thesis, Islamic Azad University of Tehran, Iran, 120 pp.

Berktold A.; 1983: *Electromagnetic studies in geothermal regions*. Geophys. Surv., **6**, 173-200.

Caldwell T.G., Bibby H.M. and Brown C.; 2004: *The magnetotelluric phase tensor.* Geophys. J. Int., **158**, 457-469.

Campbell D.L.; 1978: *Investigation of the stress concentration mechanism for interpolate earthquakes*. Geophys. Res. Lett., **5**, 477-479, doi:10.1029/GL005i006p00477.

Dhanunjaya Naidu G., Manoj C., Patro P., Sreedhar S. and Harinarayana T.; 2011: *Deep electrical signatures across the Achankovil shear zone, southern Granulite Terrain inferred from magnetotellurics*. Gondwana Res., **577**, 367-389.

Johnston J.M., Pellerin L. and Hohmann G.W.; 1992: *Evaluation of electromagnetic methods for geothermal reservoir detection*. Geotherm. Resour. Counc. Trans., **16**, 241-245.

Jones A.G.; 1993: *Electromagnetic images of modern and ancient subduction zones: plate tectonic signatures in the continental lithosphere*. Tectonophys., **219**, 29-45.

Jones A.G. and Dumas I.; 1993: *Electromagnetic images of a volcanic zone*. Phys. Earth Planet. Inter., **81**, 289-314.

Jones A.G., Kastube J. and Schwann P.; 1997: *The longest conductivity anomaly in the world explained: sulphides in fold hinges causing very high electrical anisotropy*. J. Geomagn. Geoelec., **49**, 1619-1629.

Jones A.G., Lezaeta P., Ferguson I.J., Chave A.D., Evans R.L., Garcia X. and Spratt J.; 2003: *The electrical structure of the Slave craton*. Lithos, **71**, 505-527.

McKenzie D.S.; 1972: *Active tectonics of the Mediterranean region*. Geophys. J. R. Astron. Soc., **30**, 109-185.

Montahaie M., Brasse H. and Oskooi B.; 2010: *Crustal conductivity structure of a margin from magnetotelluric investigations*. J. Earth Space Phys., **36**, 21-32.

Naganjaneyulu K. and Santosh M.; 2010: *The central India tectonic zone: a geophysical perspective on continental amalgamation along a Mesoproterozoic suture*. Gondwana Res., **18**, 547-564.

Oskooi B. and Darijani M.; 2013: *2D inversion of the magnetotelluric data from Mahallat geothermal field in Iran using finite element approach*. Arabian J. Geosci., doi:10.1007/s12517-013-0893-6.

Oskooi B., Pedersen L.B., Smirnov M., Árnason, K., Eysteinsson, H., Manzella A. and DGP Working Group; 2005: *The deep geothermal structure of the Mid-Atlantic Ridge deduced from MT data in SW Iceland*. Phys. Earth Planet. Inter., **150**, 183-195.

Patro P.K. and Sarma S.V.S.; 2009: *Lithospheric electrical imaging of the Deccan trapcovered region of western India*. J. Geophys. Res., **114**, B01102.

Pedersen L.B.; 2004: *Determination of the regularization level of truncated singular-value decomposition inversion: the case of 1D inversion of MT data*. Geophys. Prospect., **52**, 261-270.

Pedersen L.B. and Engels M.; 2005: *Routine 2D inversion of magnetotelluric data using the determinant of the impedance tensor*. Geophys., **70**, 33-41.

Rezaie M., Ghorbani M. and Bomeri M.; 2009: *The hydrogeology and geothermology of the Mahallat hot springs*. In: 1st National Conference on Hydrogeology, Behbehan, Iran, extended abstract, 4 pp.

Siripunvaraporn W. and Egbert G.; 2000: *An efficient data-subspace inversion method for 2-D magnetotelluric data*. Geophys., **65**, 791-803.

Smirnov M.Yu.; 2003: *Magnetotelluric data processing with a robust statistical procedure having a high breakdown point*. Geophys. J. Int., **152**, 1-7.

Smirnov M.Yu. and Pedersen L.B.; 2009: *Magnetotelluric measurements across the Sorgenfrei-Tornquist zone in southern Sweden and Denmark*. Geophys. J. Int., **176**, 443-456.

Spichak V. and Manzella A.; 2009: *Electromagnetic sounding of geothermal zones*. J. Appl. Geophys., **68**, 459-478.

Swift C.M.; 1967: *A magnetotelluric investigation of electrical conductivity anomaly in the southwestern United States*. PhD Thesis, Massachusetts Institute of Technology, Cambridge, MA, USA, 211 pp.

Unsworth M.; 2010: *Magnetotelluric studies of active continent-continent collisions*. Surv. Geophys., **31**, 137-161, doi:10.1007/s10712-009-9086-y.

Unsworth M.J., Egbert G.D. and Booker J.R.; 1999: *High resolution electromagnetic imaging of the San Andreas fault in central California*. J. Geophys. Res., **104**, 1131-1150.

Unsworth M.J., Malin P.E., Egbert G.D. and Booker J.R.; 1997: *Internal structure of the San Andreas fault zone at Parkfield, California*. Geol., **25**, 359-362.

Wannamaker P.E., Booker J.R., Jones A.G., Chave A.D., Filloux J.H., Waff H.S. and Law L.K.; 1989: *Resistivity cross-section through the Juan de Fuca subduction system and its tectonic implications*. J. Geophys. Res., **94**, 14121-14125.

Corresponding author: Behrooz Oskooi
Department of Geomagnetism, Institute of Geophysics, University of Tehran
Kargar shomali, Tehran, Iran
Phone: +98 21 61118238; fax: +98 21 88009560; e-mail: boskooi@ut.ac.ir